GENERATION OF ATTOSECOND X-RAY PULSE THROUGH COHERENT RELATIVISTIC NONLINEAR THOMSON SCATTERING

Kitae Lee[*†], Seong Hee Park, Yong-Ho Cha, Young Uk Jeong, and Byung Cheol Lee
KAERI, Daejon, Korea

Abstract

The nonlinear Thomson scattered radiation, which is generated by irradiating an intense laser pulse on an electron beam, was investigated both in analytical and numerical ways. The condition under which the scattered radiations from different electrons coherently superposed was analytically obtained and the effects of electron beam parameters on coherent harmonic spectrum were investigated. The condition shows that very short bunch length of a few 10 nm and small beam diameter of a few 10 μm are required with typical beam parameters of 0.1 % energy spread and 1 mrad beam divergence. To observe the effect of finite laser beam size on the scattered radiation a numerical simulation was performed with a Gaussian laser beam.

INTRODUCTION

The generation of ultrashort radiation pulse has been attracted much interesting since it could be a unique tool to investigate ultra-fast dynamics in nature, such as motions of electrons in atoms or nucleons in atomic nuclei. The advent and development of CPA (Chirped-Pulse Amplification) technology [1] has opened the world of femtosecond. Currently an ultra-intense laser pulse, which becomes realized due to the CPA technology, makes it possible to generate an attosecond radiation pulse.

Several mechanisms, which exploits harmonic radiations have been proposed and/or demonstrated [2]. The train of a few 100 attosecond pulse has been observed in the case of laser-noble gas interaction [3-5].

In the case of the laser-noble gas interaction, the harmonic radiations are generated by nonlinear interaction of ionized electrons driven by laser pulse with atomic ions. Instead, the nonlinear Thomson scattering exploits relativistic nonlinear oscillatory motion of electron irradiated by an ultra-intense laser pulse. When the strength of laser pulse, represented by the following normalized vector potential,

$$a_o = 8.5 \times 10^{-10} \lambda[\mu m] I[W/cm^2]^{1/2}, \qquad (1)$$

is much smaller than unity, the electron undergoes simple harmonic oscillation, thus radiating same frequency. As a_o gets larger than unity, the motions of electrons become relativistic nonlinear resulting in harmonic radiation, which is called RNTS (Relativistic Nonlinear Thomson Scattered) radiation.

[*] klee@kaeri.re.kr

The characteristics of such RNTS have been numerically investigated [6-7] and it has been shown that the radiations from a group of electrons can be coherently superposed with an ultra-thin target of a few 10 nm, resulting in an intense, ultra-short pulse of a few 10 attosecond [8].

In the case of solid target, even though the plasma effect can be neglected by using an ultra-thin target, much thinner than plasma skin depth, the strong electrostatic field by charge separation could degrade the coherent RNTS radiation. Such a plasma effect could be avoided by using a relativistic electron beam as a target. Another advantage using a relativistic electron beam is that the radiation intensity increases as the beam energy increases.

With an approximation of a small beam energy spread and a beam divergence, an analytic formula to describe the scattered radiation from electrons irradiated by a planewave laser filed is obtained including an initial electron distribution. By using it, the condition for the scattered radiation to be coherent was obtained and its dependence on the beam parameters was investigated observing harmonic spectrum. The effect of a finite laser beam size was also investigated through a numerical simulation.

COHERENT CONDITION: FORMALISM

In the planewave approximation, the dynamics of an electron under a laser pulse can be analytically obtained [9]. Then by using Lienard-Wiechert potential [10], the angular spectral intensity can be obtained as,

$$\frac{d^2 I}{d\alpha\, d\Omega} = 2\left|\vec{A}(\omega)\right|^2, \qquad (2)$$

where, the radiation field, $\vec{A}(\omega)$ including all the electrons is approximately written as,

$$\vec{A}(\omega) \approx NF(\omega)\vec{A}_o(\omega),$$
$$\vec{A}_o(\omega) = \sqrt{\frac{e^2}{2\pi^2 c}} \frac{\omega}{\omega_o} \varphi_o \sum_m \left(R_\theta^{(m)}\hat{e}_\theta + R_\phi^{(m)}\hat{e}_\phi\right) \qquad (3)$$

Figure 1 Schematic geometry for the scattering process.

In above equation, N is the number of electrons, $\vec{A}_o(\omega)$ the scattered radiation field from an electron having central velocity [9], and $F(k)$ a coherent factor for an initial distribution of electrons (Fig. 1). For a Gaussian electron beam, $F(k)$ can be written as,

$$F(k) = \frac{1}{\sqrt{1+k^2 l'^2}} \times$$

$$\exp\left[-\frac{1}{2}\frac{k^2}{1+k^2l'^2} \times \left\{ \begin{array}{c} l^2 N_{gz}^2 + R^2\left(N_{gx}^2 + N_{gy}^2\right) \\ + k^2 R^2 T^2 \left(\begin{array}{c} l^2\left(N_{gx}n_{gz} - N_{gz}n_{\theta gz}\right)^2 \\ + \left(R^2 n_{\theta gz}^2 + l^2 n_{gz}^2\right)N_{gy}^2 \end{array} \right) \end{array} \right\} \right] \quad (4)$$

$N_{oz} = \hat{n}\cdot\hat{n}_o - p_o n_{oz}, N_{ox} = \hat{n}\cdot\hat{n}_{\theta o} - p_o n_{\theta oz}, N_{oy} = \hat{n}\cdot\hat{n}_{\phi o},$

$N_{gz} = \hat{n}\cdot\hat{n}_g - p_o n_{gz}, N_{gx} = \hat{n}\cdot\hat{n}_{\theta g} - p_o n_{\theta gz}, N_{gy} = \hat{n}\cdot\hat{n}_{\phi g},$

$p_o = \frac{1-\vec{\beta}_o\cdot\hat{n}}{1-\beta_{oz}}, w_o = \frac{\beta_o}{1-\beta_{oz}}$

$T^2 = w_o^2\left(\frac{\sigma_\Gamma^2}{(\gamma^2-1)^2}N_{oz}^2 + \sigma_{\beta'}^2\left(N_{ox}^2 + N_{oy}^2\right)\right)$

$l'^2 = T^2\left(l^2 n_{gz}^2 + R^2 n_{\theta gz}^2\right)$

where c_Γ, $c_{\beta'}$, l, and R are beam energy spread in fraction, beam divergence, length, and radius, respectively. In deriving Eq. (4), different directions between beam direction ($\hat{n}_o$) and normal to beam front ($\hat{n}_g$) were used. The coherent factor shows that as the beam parameters get larger, the angular spectral intensity decreases from the high energy part.

The scattered radiations from an electron beam to be coherent, above coherent factor should be almost 1, or the exponent should approach to zero up to a frequency a_c. In the x-z plane, $N_{gy} = 0$, then above requirement leads to the following relations between angles,

$$N_{gx} = \sin(\theta - \theta_g) + \sin\theta_g \frac{1 - \beta_o\cos(\theta_o - \theta)}{1 - \beta_o\cos\theta_o} = 0, \quad (5)$$

and restrictions on the beam parameters as

$$\frac{k_c^2 l^2 N_{gz}^2}{1+k^2 l'^2}\left(1 + k^2 R^2 T^2 n_{\theta gz}^2\right) < 1. \quad (6)$$

The physical meaning of Eqs. (5) and (6) is that time delays between electrons should be less than the pulse width generated by a single electron [8].

CHARACTERISTICS OF NONLINEAR THOMSON SCATTERED RADIATION

In the case of circularly polarized laser pulse, the radiation characteristics of nonlinear Thomson scattering by a single electron was investigated through analytic formula on x-z plane. Fig. 2 shows peak radiation direction (angle) and its intensity (radius) on electron direction (θ_o) for $a_o = 3$ and $\gamma_o = 10$.
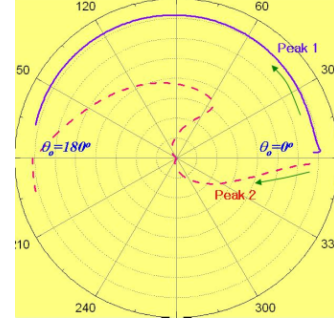
Figure 2 For $a_o = 3$ and $\gamma_o = 10$, peak radiation directions and its intensities on initial electron direction. The arrows show that how the two peak (see Fig. 3) directions vary as the electron's direction varies.

When $\theta_o = 0^o$, two peak appears symmetric on z-axis. As the θ_o increases in the forward scattering regime, the peak at positive moves with electron's direction but the one at negative the other direction (Fig. 3 (a)). And in the backward scattering regime, the two peaks become near symmetric on the direction of electron velocity (Fig. 3(b)). The harmonic spectrum at the peak direction for Figs. 3 (a) and (b) are plotted in (c) and (d), respectively. The spectral range in the case of a forward scattering shows no relativistic Doppler shift, but in the backward direction, due to relativistic Doppler shift, much higher photons are radiated.
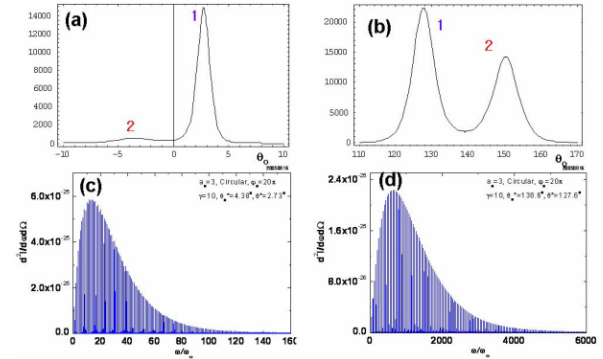

Figure 3 Angular distributions of radiation intensity for (a) $\theta_o = 4.38^o$ and (b) $\theta_o = 138.6^o$. The (c) and (d) show angular spectra at peak 1 for the conditions of (a) and (b) respectively.

The dependence of peak directions and its peak spectral intensities on the relativistic gamma factor are plotted in Fig. 4. For small γ, forward radiation has higher intensity. But as the electron's energy increases, backward scattering becomes dominant due to its additional relativistic Doppler effect, which scales as γ^2. Thus for large γ, the intensity in backward scattering scales to $\sim \gamma^4$, while forward scattering to $\sim \gamma^2$.
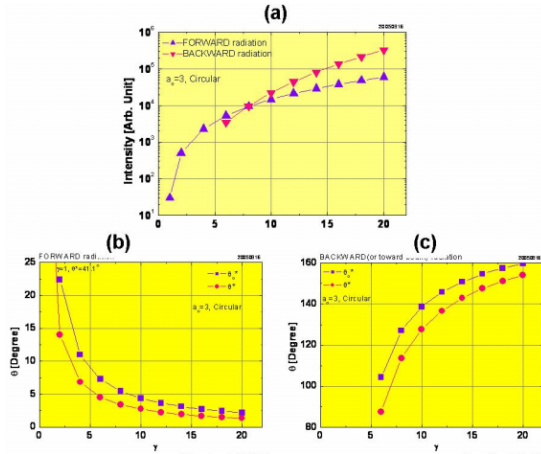
Figure 4 For $a_o = 3$ and $\gamma_o = 10$, the variations of peak angular intensities are plotted in (a) for both forward and backward directions and directions are plotted in (b) and (c) for forward and backward scattering, respectively.

COHERENT RADIATION ON BEAM PARAMETERS

In the study of a single electron case, it was found that there are two cases for high peak intensity, one forward and the other backward scattering. In the case of backward scattering, it has higher intensity and higher spectral range, which are usually adopted in the case of linear Compton scattering. But in the sense of coherent radiation for the generation of ultra-short radiation pulse, forward scattering has better characteristics to be realized. It is easy to satisfy the angular condition (Eq. (5)), or to find the direction of beam front (θ_g) for both cases. However in case of the backward scattering, since N_{gz} and k_c have much higher values than in the case of the forward scattering, Eq. (6) requires much difficult beam conditions. Thus for the coherent radiation to generate ultra-short radiation pulse, the forward scattering can be adopted.
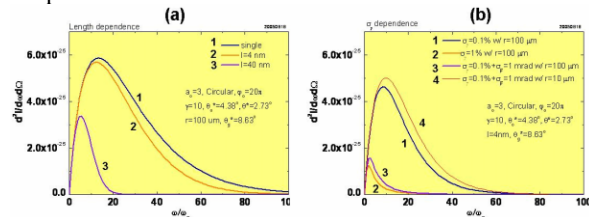
Figure 5 The variation of angular spectral intensity on (a) beam length and (b) energy spread and beam divergence. For convenience, only envelopes are plotted.

For the case of Fig. 3 (c), the coherent condition for angle (Eq. (5)) gives $\theta_g = 8.63^o$ and Eq. (6) restricts the beam length to a few nanometer if $T = 0$. In Fig. 5 (a) the variation of angular spectral intensity on the beam length are plotted. With 4 nm beam length (curve 2 in Fig. 5(a)), it shows almost same spectral shape with single electron's (curve 1 in Fig. 5(a)), which corresponds to

~10 attosecond pulse width. When the beam length increases to 40 nm (curve 3 in Fig. 5(a)), the spectral intensity at high energy is much decreases as expected from Eq. (4). However the spectral broadening is still enough to generate a few 10 attosecond pulse. In addition to length and 100 µm beam radius, effects on other parameters can be seen from Fig. 5 (b). With 0.1 % energy spread (Curve 1 in Fig. 5 (b)), which is typical for an electron beam, the spectrum decreases by a factor of 2/3 in both intensity and spectral range. It has found that the beam divergence is most critical factor to keep the radiation coherent. With 1 mrad beam divergence in addition to 0.1 % energy spread (Curve 3 in Fig. 5 (b)), the spectrum is much reduced by a factor of 5. When there is no energy spread and beam divergence, beam radius does not affect the coherent spectrum. However with finite energy spread and beam divergence, the radius becomes also critical values. When the radius is reduced by a factor of 10 compared with curve 2 in Fig. 5 (b) (Curve 4 in Fig. 5 (b)), the effect of such beam parameters can be avoided.

EFFECT OF FINITE LASER BEAM

In above analytical study, the planewave approximation has been adopted, since the quivering amplitude of oscillating electron (<1 µm) is much smaller than a typical laser focal size (> 10 µm). However to address such an effect more quantitatively, a numerical study [7] was performed. The finite laser beam size could affect the scattered radiation through electron's dynamics in two ways. One is the alteration of dynamics as an electron oscillates off the laser axis and the other is different dynamics between electrons at different initial positions.
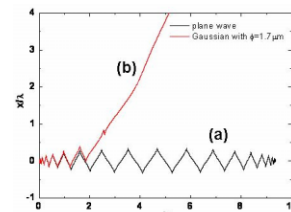

Figure 6 Orbits of an electron for (a) planewave and (b) paraxial Gaussian wave with a beam diameter of 1.7 µm. A linearly polarized laser pulse with 10^{19} W/cm^2 was used for this calculation.

With a finite laser beam, or a paraxial Gaussian beam, the electron can escape from the laser axis once the quivering amplitude becomes comparable with beam radius (Fig. 6 (b)). Then no more scattered radiation could be generated. In Fig. 7, the scattered angular radiation powers between planewave and Gaussian wave with a beam diameter of 24 µm are compared. First, the lack of radiation power at later times for a Gaussian beam can be understood from Fig. 6. And much lower power and much broadened pulse shape is considered to be caused by the second effect commented in previous paragraph.
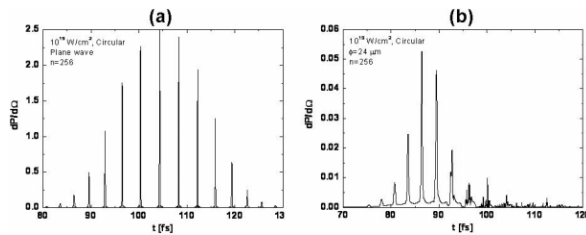
Figure 7 Scattered angular radiation powers for (a) planewave and (b) Gaussian wave with a beam diameter of 24 μm. A circularly polarized laser pulse with 10^{19} W/cm^2 and 256 electrons are used in this calculation.

CONCLUSION

Analytical formulas to describe scattered radiation by interaction of a planewave laser pulse with an electron beam was developed, which include electron beam parameters. The nonlinear Thomson scattering was investigated which has very interesting angular distributions. Using the derived formulas, the condition for the coherent nonlinear Thomson scattering was obtained and its dependence on the beam parameters was observed. The effect of Gaussian laser beam was studied by a numerical method. This analysis shows that to make the nonlinear Thomson scattered radiation be coherent with an electron beam, a very small sized electron beam with a large laser beam size are required.

REFERENCES

[1] M. D. Perry and G. Mourou, Science **264**, 917 (1004).
[2] Pierre Agostini and Louis F DiMauro, Rep. Pro. Phys. **67**, 813 (2004).
[3] P. M. Paul et al., Science **292**, 1689 (2001).
[4] E. Hertz et al., Phys Rev A **64**, 051801 (2001)..
[5] M. Hentschel et al., Nature **414**, 509 (2001).
[6] K. Lee et al., Opt. Express 11, 309 (2003).
[7] K. Lee et al., Phys. Rev. E **67**, 026502 (2003).
[8] K. Lee et al., Phys. Plasmas **12**, 043107 (2005).
[9] E. Esarey et al., Phys. Rev. E **48**, 3003 (1993).
[10] J. D. Jackson, *Classical Electrodynamics* 2nd ed. Chap. 14 (John Wiley and Sons, New York, 1975).